



only be attributed to the popularity bias [2], which could actually lead to negative user preference. These interactions can be considered as *noisy-positive* examples [17, 24, 38]. Besides, a missing interaction could also be attributed to unawareness of the user because the item is not exposed to this user. Such *noisy-negative* examples could have signalled potential positive user preferences. The normal training procedure overlooks these noisy examples, leading to misunderstanding of the real user preference and sub-optimal recommendation [2, 38].

To denoise implicit feedback, some recent efforts have been done by using re-sampling methods [5, 7, 9, 42] or re-weighting methods [34]. Re-sampling methods focus on designing more effective samplers. For example, [9] considers that the missing interactions of popular items are highly likely to be real negative examples. However, the performance of re-sampling methods depends heavily on the sampling distribution and suffers from high variance [44]. [34] proposed a re-weighting method which assigns lower weights or zero weights to high-loss samples since the noisy examples would have higher losses. However, [31] shows that hard yet clean examples also tend to have high losses. As a result, [34] could encounter difficulties to distinguish between hard clean and noisy examples. Besides, some research focuses on utilizing auxiliary information to denoise implicit feedback [20, 23, 25, 41] but this kinds of methods need additional input.

In this work, we propose probabilistic and variational denoising for implicit feedback recommendation without using additional data. The signal for denoising comes from an insightful observation: different models tend to make relatively similar predictions for clean examples which represent the real user preference, while predictions for noisy examples would vary much more among different models. This observation is substantiated in an empirical study described in the next section. To this end, we propose *denoising with probabilistic inference* (DPI) which aims to minimize the Kullback–Leibler (KL) divergence between the real user preference distributions parameterized by two recommendation models, and meanwhile, maximize the likelihood of the data observation given the real user preference. DPI can be considered as a learning framework which incorporates the weakly supervised signals from different model predictions to denoise the target recommender. We then show that DPI recovers the evidence lower bound (ELBO) of a variational auto-encoder (VAE) in which the real user preference acts as the latent variable. This leads to the second learning framework *denoising with variational auto-encoder* (DVAE). More precisely, we use a pretrained model to describe the prior distribution. Then the target recommendation model which is used to infer user preferences and then generate final recommendation acts as the encoder, while the decoder will fit the likelihood of data observation given the real user

preference. The proposed DPI and DVAE act as two denoising learning frameworks and can be naturally incorporated with existing recommendation models.

To summarize, the main contributions of this work are as follow:

- We find that the different models tend to make more similar predictions for clean examples than for noisy ones. This observation provides new hints to devise denoising methods for implicit feedback recommendation.
- We propose two learning frameworks DPI and DVAE which utilize the difference between model predictions as the denoising signal for implicit feedback and infer the real user preference from corrupted binary data.
- We instantiate DPI and DVAE with four state-of-the-art recommendation models and conduct extensive experiments on three datasets. The results demonstrate the effectiveness of our proposed methods.

## 2 Motivation

According to the theory of robust learning [12, 19], noisy examples tend to have relatively high loss values. However, the hard yet clean examples which fall near the classification boundary also have high losses [31]. These hard clean examples play an important role to boost the recommendation performance of implicit feedback [6, 37, 43]. Denoising methods based on loss values could encounter difficulties to distinguish between noisy examples and hard clean examples, leading to sub-optimal solutions. However, we find that another signal which can help to identify noisy examples can be obtained from the comparison between different model predictions.

To illustrate such signal, we conduct an empirical study on the Modcloth dataset<sup>1</sup>, which comes from an e-commerce website selling women’s clothing and accessories. We train four notable recommendation models (i.e. MF [21], GMF and NeuMF [14] and LightGCN [13]) with the binary user-item implicit feedback with the normal training assumption (i.e., all interacted items are considered as positive examples and negative examples are sampled from missing interactions, as shown in Figure 1(a)). Figure 2(a) shows the mean prediction differences between two different models on clean positive examples and noisy positive examples.

More precisely, we consider interactions whose ratings are 4 and 5 as clean positive examples while interactions whose ratings are 1 and 2 as noisy positive examples. The difference is defined as  $|I(\delta(y_{ui})) - I(\delta(y'_{ui}))|$ , where  $y_{ui}$  and  $y'_{ui}$  are the predicted scores from two models regarding user  $u$  and item  $i$ ,  $\delta$  is the sigmoid function.  $I(x)$  is an indicator function and is defined as  $I(x) = 1$  when  $x \geq 0.5$  and  $I(x) = 0$  otherwise. We calculate all prediction differences on clean examples and noisy examples respectively and then report the average. It’s obvious that the model prediction differences on noisy

<sup>1</sup><https://github.com/MengtingWan/marketBias>

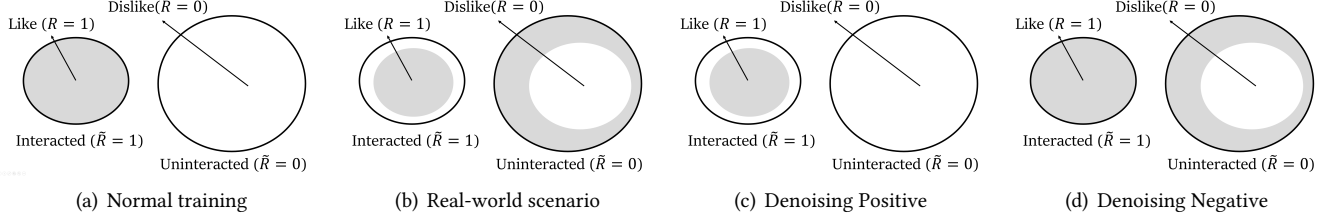


**Figure 1.** Different assumptions in recommendation training on implicit feedback. Gray denotes positive user preference (i.e., ‘like’) while white denotes negative preference (i.e., ‘dislike’). In normal training, interacted instances are considered as positive examples and uninteracted ones are considered as negative examples, as shown in (a). However, in real-world applications, there are both noisy-positive examples in interacted items and noisy-negative examples in uninteracted items, as shown in (b). (c) denotes only denoising positive examples [25, 34], while (d) only denoises negative examples [5, 42].

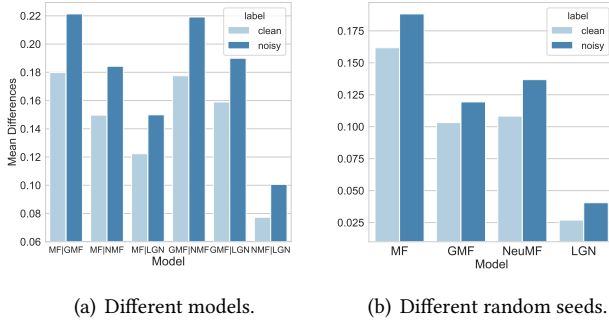


**Figure 2.** Mean prediction differences on **clean** and **noisy** examples in Modcloth from (a) different models or (b) one model trained with two different random seeds. NMF and LGN is short for NeuMF and LightGCN respectively.

examples are significantly larger than the differences on clean examples. In other words, *different models tend to make relatively similar predictions for clean examples compared with noisy examples*. That is to say, different models tend to fit different parts of the corrupted data but clean examples are the robust component which every model attempts to fit. This observation also conforms with the nature of robust learning. Besides, we also find that even one model trained on the same dataset with different random seeds tends to make more consistent predictions on clean examples compared with noisy examples, as shown in Figure 2(b).

### 3 METHOD

In this section, we propose two learning frameworks: DPI and DVAE, using the observations described in section 2 as the weakly supervised signals to denoise implicit feedback for recommendation. Before detailed description of these methods, some notations and problem formulation are given.

#### 3.1 Notations and Problem Formulation

We use  $u \in \mathcal{U}$  and  $i \in \mathcal{I}$  to denote the user and item with  $\mathcal{U}$  and  $\mathcal{I}$  being the user and item sets respectively.  $\tilde{\mathbf{R}} \in \mathbb{R}^{|\mathcal{U}| \times |\mathcal{I}|}$  is the binary matrix for corrupted data.  $\tilde{r}_{ui}$  represents the  $(u, i)$ -th entry of  $\tilde{\mathbf{R}}$  and is defined as  $\tilde{r}_{ui} = 1$  if there is an

interaction between user  $u$  and item  $i$ , otherwise  $\tilde{r}_{ui} = 0$ . Due to the existence of noisy examples, the real preference matrix is different from  $\tilde{\mathbf{R}}$ . We use  $\mathbf{R} \in \mathbb{R}^{|\mathcal{U}| \times |\mathcal{I}|}$  to denote the real preference matrix and  $r_{ui}$  is the real preference of user  $u$  over item  $i$ . What we have is the corrupted binary  $\tilde{\mathbf{R}}$  while the clean  $\mathbf{R}$  is not accessible.

Formally, we assume  $r_{ui}$  is drawn from a Bernoulli distribution:

$$r_{ui} \sim \text{Bernoulli}(\eta_{ui}) \approx \text{Bernoulli}(f_{\theta}(u, i)), \quad (1)$$

where  $\eta_{ui}$  describes the probability of positive preference (i.e.,  $r_{ui} = 1$ ) and is approximated by  $f_{\theta}(u, i)$ .  $\theta$  denotes the parameters of  $f$ . We use  $f_{\theta}$  as our target recommender that generates final recommendation. Generally speaking,  $f_{\theta}$  is expected to have high model expressiveness. Since the denoising signal comes from the comparison between different model predictions, we introduce another auxiliary Bernoulli distribution parameterized by  $g_{\mu}(u, i)$ . In this paper, we use a relatively simple model matrix factorization (MF) [21] as the auxiliary model  $g_{\mu}$ . Recent research has demonstrated that MF is still one of the most effective model to capture user preference for recommendation [29].

Considering both the noisy positive and noisy negative examples, we assume that given the real preference  $r_{ui}$ , the corrupted binary  $\tilde{r}_{ui}$  is also drawn from Bernoulli distributions as

$$\begin{aligned} \tilde{r}_{ui} | r_{ui} = 0 &\sim \text{Bernoulli}(h_{\phi}(u, i)) \\ \tilde{r}_{ui} | r_{ui} = 1 &\sim \text{Bernoulli}(h'_{\psi}(u, i)), \end{aligned} \quad (2)$$

where  $h_{\phi}(u, i)$  and  $h'_{\psi}(u, i)$  are two models describing the probability, parameterized by  $\phi$  and  $\psi$ , respectively. We use two MF models as  $h$  and  $h'$  without special mention.

The task of this paper is, given the corrupted binary data  $\tilde{\mathbf{R}}$ , to infer the real user preference  $\mathbf{R}$  and its underlying model  $f_{\theta}$ , then to use  $f_{\theta}$  to generate recommendation.

#### 3.2 Denoising with Probabilistic Inference

As discussed in section 2, for clean examples which denote the real user preference, different models tend to make

more consistent predictions compared with noisy examples. For simplicity, in this subsection we use  $P(\mathbf{R})$  to denote the real user preference  $Bernoulli(\eta)$ .  $P_f(\mathbf{R})$  and  $P_g(\mathbf{R})$  are used to represent the approximated  $Bernoulli(f_\theta)$  and  $Bernoulli(g_\mu)$ , correspondingly.

Due to the fact that  $P_f(\mathbf{R})$  and  $P_g(\mathbf{R})$  both approximate the real user preference  $\mathbf{R}$ , they should remain a relatively small KL-divergence according to section 2, which is formulated as

$$D[P_g(\mathbf{R})||P_f(\mathbf{R})] = E_{\mathbf{R} \sim P_g} [\log P_g(\mathbf{R}) - \log P_f(\mathbf{R})]. \quad (3)$$

However, naively optimizing Eq.(3) is meaningless since we do not have the supervision signal of  $\mathbf{R}$ . As a result, we need to introduce supervision signals from the corrupted data  $\tilde{\mathbf{R}}$ . Using the Bayes theorem,  $P_f(\mathbf{R})$  can be approximated as

$$P_f(\mathbf{R}) \approx P(\mathbf{R}) = \frac{P(\tilde{\mathbf{R}})P(\mathbf{R}|\tilde{\mathbf{R}})}{P(\tilde{\mathbf{R}}|\mathbf{R})}. \quad (4)$$

Combining Eq.(4) and Eq.(3), we can obtain

$$\begin{aligned} D[P_g(\mathbf{R})||P_f(\mathbf{R})] &= E_{\mathbf{R} \sim P_g} [\log P_g(\mathbf{R}) - \log P_f(\mathbf{R})] \\ &\approx E_{\mathbf{R} \sim P_g} [\log P_g(\mathbf{R}) - \log \frac{P(\tilde{\mathbf{R}})P(\mathbf{R}|\tilde{\mathbf{R}})}{P(\tilde{\mathbf{R}}|\mathbf{R})}] \\ &= E_{\mathbf{R} \sim P_g} [\log P_g(\mathbf{R}) - \log P(\mathbf{R}|\tilde{\mathbf{R}}) - \log P(\tilde{\mathbf{R}}) + \log P(\tilde{\mathbf{R}}|\mathbf{R})] \\ &= D[P_g(\mathbf{R})||P(\mathbf{R}|\tilde{\mathbf{R}})] - \log P(\tilde{\mathbf{R}}) + E_{\mathbf{R} \sim P_g} [\log P(\tilde{\mathbf{R}}|\mathbf{R})]. \end{aligned} \quad (5)$$

We then rearrange the terms in Eq.(5) and obtain

$$\begin{aligned} E_{\mathbf{R} \sim P_g} [\log P(\tilde{\mathbf{R}}|\mathbf{R})] - D[P_g(\mathbf{R})||P_f(\mathbf{R})] \\ = \log P(\tilde{\mathbf{R}}) - D[P_g(\mathbf{R})||P(\mathbf{R}|\tilde{\mathbf{R}})]. \end{aligned} \quad (6)$$

We can see the meaning of maximizing the left side of Eq.(6) is maximizing the likelihood of data observation given real user preference (i.e.,  $\log P(\tilde{\mathbf{R}}|\mathbf{R})$ ) and meanwhile minimizing the KL-divergence between two models which both approximate the real user preference (i.e.,  $D[P_g(\mathbf{R})||P_f(\mathbf{R})]$ ). Since the KL-divergence  $D[P_g(\mathbf{R})||P(\mathbf{R}|\tilde{\mathbf{R}})]$  is larger than zero, the left side of Eq.(6) can also be seen as the lower bound of  $\log P(\tilde{\mathbf{R}})$ . The bound is satisfied only if  $P_g(\mathbf{R})$  perfectly recovers  $P(\mathbf{R}|\tilde{\mathbf{R}})$ , in other words,  $P_g(\mathbf{R})$  perfectly approximates the real user preference distribution given the corrupted data.

A naive solution is to directly maximize the left side of Eq.(6) with an end-to-end fashion. However, it would not yield satisfactory performance. The reason is that the left side of Eq.(6) is based on the expectation over  $P_g$ . The learning process is equivalent to training  $g_\mu$  with the corrupted data  $\tilde{\mathbf{R}}$  and then uses  $D[P_g(\mathbf{R})||P_f(\mathbf{R})]$  to transmit the information from  $g_\mu$  to  $f_\theta$ . However, the information is corrupted and it will affect the performance of our target model  $f_\theta$ . To fix the problem, we notice that when the training process is converged, two distributions  $P_f(\mathbf{R})$  and  $P_g(\mathbf{R})$  would be

close to each other. We can then modify the left side of Eq.(6) as

$$\begin{aligned} E_{\mathbf{R} \sim P_f} [\log P(\tilde{\mathbf{R}}|\mathbf{R})] - D[P_g(\mathbf{R})||P_f(\mathbf{R})] \\ \approx \log P(\tilde{\mathbf{R}}) - D[P_g(\mathbf{R})||P(\mathbf{R}|\tilde{\mathbf{R}})]. \end{aligned} \quad (7)$$

Then optimizing the left side of Eq.(7) is actually training  $f_\theta$  with the corrupted  $\tilde{\mathbf{R}}$  and then transmit information to  $g_\mu$ . However, since  $g_\mu$  is relatively simple than  $f_\theta$ ,  $g_\mu$  could only fit the robust data component (i.e., clean examples). Thus  $g_\mu$  would not affect the learning of  $f_\theta$  on clean examples, while in the meantime, pull back  $f_\theta$  on noisy samples, or in other words, downgrade the noisy signal. To this end, the denoising objective function can be formulated as

$$\mathcal{L} = -E_{\mathbf{R} \sim P_f} [\log P(\tilde{\mathbf{R}}|\mathbf{R})] + D[P_g(\mathbf{R})||P_f(\mathbf{R})]. \quad (8)$$

Considering that the gradient of  $D[P_g||P_f]$  and  $D[P_f||P_g]$  to  $\theta$  is different, which could slightly affect the performance, we then formulate the final denoising objective function of DPI as

$$\mathcal{L}_{DPI} = -E_{\mathbf{R} \sim P_f} [\log P(\tilde{\mathbf{R}}|\mathbf{R})] + \alpha D[P_g||P_f] + (1-\alpha) D[P_f||P_g], \quad (9)$$

where  $\alpha \in [0, 1]$  is a hyper-parameter.

More precisely, we can give the detailed formulation of the term  $E_{\mathbf{R} \sim P_f} [\log P(\tilde{\mathbf{R}}|\mathbf{R})]$  in  $\mathcal{L}_{DPI}$  as

$$\begin{aligned} E_{\mathbf{R} \sim P_f} [\log P(\tilde{\mathbf{R}}|\mathbf{R})] &= \sum_{(u,i)} E_{r_{ui} \sim P_f} [\log P(\tilde{r}_{ui}|r_{ui})] \\ &= \sum_{(u,i)|\tilde{r}_{ui}=1} \left\{ \begin{aligned} &\log P(\tilde{r}_{ui}=1|r_{ui}=1) \cdot P_f(r_{ui}=1) \\ &+ \log P(\tilde{r}_{ui}=1|r_{ui}=0) \cdot P_f(r_{ui}=0) \end{aligned} \right\} \\ &+ \sum_{(u,i)|\tilde{r}_{ui}=0} \left\{ \begin{aligned} &\log P(\tilde{r}_{ui}=0|r_{ui}=1) \cdot P_f(r_{ui}=1) \\ &+ \log P(\tilde{r}_{ui}=0|r_{ui}=0) \cdot P_f(r_{ui}=0) \end{aligned} \right\} \\ &= \sum_{(u,i)|\tilde{r}_{ui}=1} \log h'_\psi(u, i) \cdot f_\theta(u, i) + \log h_\phi(u, i) \cdot (1 - f_\theta(u, i)) \\ &+ \sum_{(u,i)|\tilde{r}_{ui}=0} \log(1 - h'_\psi(u, i)) \cdot f_\theta(u, i) + \log(1 - h_\phi(u, i)) \cdot (1 - f_\theta(u, i)). \end{aligned} \quad (10)$$

The KL divergence term  $D[P_g||P_f]$  can be calculated as

$$D[P_g||P_f] = g_\mu(u, i) \cdot \log \frac{g_\mu(u, i)}{f_\theta(u, i)} + (1 - g_\mu(u, i)) \cdot \log \frac{1 - g_\mu(u, i)}{1 - f_\theta(u, i)}.$$

$D[P_f||P_g]$  is computed similarly with  $D[P_g||P_f]$ .

### 3.3 Denoising with Variational Autoencoder

In last subsection, we devise the learning framework DPI. DPI utilizes an auxiliary model  $g_\mu$  as an information filter which helps to downgrade the noisy signal. As discussed before, the left side of Eq.(6) is the lower bound of  $\log P(\tilde{\mathbf{R}})$ , which is satisfied when  $P_g(\mathbf{R})$  perfectly recover  $P(\mathbf{R}|\tilde{\mathbf{R}})$ . DPI utilizes an auxiliary MF model to approximate  $P(\mathbf{R}|\tilde{\mathbf{R}})$  which has limited model capability, while in this subsection, we propose to use the more complex target recommendation



model  $f_\theta$  to approximate  $P(\mathbf{R}|\tilde{\mathbf{R}})$ . To this end, we modify the assumption of Eq.(1) as

$$r_{ui}|\tilde{r}_{ui} \sim \text{Bernoulli}(\eta_{ui}) \approx \text{Bernoulli}(f_\theta(u, i)). \quad (11)$$

We use  $Q_f(\mathbf{R}|\tilde{\mathbf{R}})$  to represent the distribution of  $\mathbf{R}|\tilde{\mathbf{R}}$  parameterized by  $f_\theta$ . Then we replace  $P_g(\mathbf{R})$  in the right side of Eq.(6) with  $Q_f(\mathbf{R}|\tilde{\mathbf{R}})$ , and obtain the KL-divergence

$$D[Q_f(\mathbf{R}|\tilde{\mathbf{R}})||P(\mathbf{R}|\tilde{\mathbf{R}})]. \quad (12)$$

Through variational inference [16], the following equation can be deduced:

$$\begin{aligned} E_{Q_f}[\log P(\tilde{\mathbf{R}}|\mathbf{R})] - D[Q_f(\mathbf{R}|\tilde{\mathbf{R}})||P(\mathbf{R})] \\ = \log P(\tilde{\mathbf{R}}) - D[Q_f(\mathbf{R}|\tilde{\mathbf{R}})||P(\mathbf{R}|\tilde{\mathbf{R}})]. \end{aligned} \quad (13)$$

We can see that Eq.(13) is exactly the objective function of a VAE [8]. Specifically, the real user preference  $\mathbf{R}$  is the latent variables.  $Q_f(\mathbf{R}|\tilde{\mathbf{R}})$  which is parameterized by our target model  $f_\theta$  maps the corrupted data  $\tilde{\mathbf{R}}$  to the latent variables  $\mathbf{R}$  and thus can be seen as the encoder. The likelihood  $P(\tilde{\mathbf{R}}|\mathbf{R})$  describes the distribution of corrupted data  $\tilde{\mathbf{R}}$  given the real user preference  $\mathbf{R}$  and acts as the decoder. Finally,  $P(\mathbf{R})$  is the fixed prior distribution. This leads to our second proposed learning framework DVAE.

Similarly with DPI, we also incorporate the reverse KL-divergence into the DVAE objective, which finally yields:

$$\begin{aligned} \mathcal{L}_{DVAE} = -E_{Q_f}[\log P(\tilde{\mathbf{R}}|\mathbf{R})] + \alpha D[Q(\mathbf{R}|\tilde{\mathbf{R}})||P(\mathbf{R})] \\ + (1 - \alpha) D[P(\mathbf{R})||Q(\mathbf{R}|\tilde{\mathbf{R}})]. \end{aligned} \quad (14)$$

We use the encoder of this VAE to generate recommendation and the decoder to fit the likelihood. As for the prior distribution  $P(\mathbf{R})$ , we use a pretrained model  $f_{\theta'}$  which has the same structure as our target model  $f_\theta$  but is trained with different random seeds. This setting is motivated by the observation that one model trained with different random seeds tends to make high variance predictions on noisy examples but more consistent predictions on clean examples. During the training process,  $\theta'$  is freezed and will not be updated, describing the fixed prior distribution.

The difference and relationship between DPI and DVAE can be summarized as follows:

- The auxiliary model  $g_\mu$  of DPI is a simple MF while the involved  $f_{\theta'}$  in DVAE has the same structure as the target recommendation model.
- DPI co-trains the auxiliary model  $g_\mu$  with  $f_\theta$  but DVAE uses a pre-trained and fixed  $f_{\theta'}$  to describe the prior distribution.
- The denoising signal of DPI comes from the prediction difference between different models while the denoising signal of DVAE comes from the prediction difference of one model trained with different random seeds.

### 3.4 Training Routine

We can see that both the objective functions of DPI and DVAE contain the term of  $E[\log P(\tilde{\mathbf{R}}|\mathbf{R})]$ . A naive solution to optimize  $E[\log P(\tilde{\mathbf{R}}|\mathbf{R})]$  is direct performing calculation as shown in Eq.(10). However, we find that it won't yield satisfactory results. The reason is that computing  $E[\log P(\tilde{\mathbf{R}}|\mathbf{R})]$  involves updating two models  $h_\phi$  and  $h'_\psi$  simultaneously. The two models could interfere with each other. One under-trained model would prevent the other one from learning well, and vice visa. To handle this issue, we split the denoising problem into two dual tasks: *Denoising Positive* (DP) which aims to denoise the noisy positive examples from interacted samples as shown in Figure 1(c); and *Denoising Negative* (DN) which aims to denoise noisy negative examples from sampled missing interactions as illustrated in Figure 1(d). We then optimize these two sub-tasks iteratively.

**3.4.1 Denoising Positive.** In this situation, we only focus on denoising noisy positive examples, which means we will regard every negative sample as a clean example, as shown in Figure 1(c). That is to say, given  $r_{ui} = 1$  we will always have  $\tilde{r}_{ui} = 1$  (i.e.,  $h'_\psi(u, i) = 1$ ). Thus in this sub-task, only the model  $h_\phi$  will be trained. Then the term  $E[\log P(\tilde{\mathbf{R}}|\mathbf{R})]$  becomes

$$\begin{aligned} E[\log P(\tilde{\mathbf{R}}|\mathbf{R})] = \sum_{(u,i)|\tilde{r}_{ui}=1} \log h_\phi(u, i) \cdot (1 - f_\theta(u, i)) \\ - \sum_{(u,i)|\tilde{r}_{ui}=0} C_1 \cdot f_\theta(u, i) + \log(1 - h_\phi(u, i)) \cdot (1 - f_\theta(u, i)), \end{aligned} \quad (15)$$

where  $C_1$  is a large positive hyperparameter to substitute  $-\log(1 - h'_\psi(u, i))$ .

**3.4.2 Denoising Negative.** In this sub-task, we only focus on denoising noisy negative examples in the sampled missing interactions, which means that we will regard every positive examples as a clean example, as shown in Figure 1(d). That is to say, given  $r_{ui} = 0$  we will always have  $\tilde{r}_{ui} = 0$  (i.e.,  $h_\phi(u, i) = 0$ ). Thus in this sub-task, only model  $h'_\psi$  will be trained. The term  $E[\log P(\tilde{\mathbf{R}}|\mathbf{R})]$  is expanded as

$$\begin{aligned} E[\log P(\tilde{\mathbf{R}}|\mathbf{R})] = \sum_{(u,i)|\tilde{r}_{ui}=0} \log(1 - h'_\psi(u, i)) \cdot f_\theta(u, i) \\ + \sum_{(u,i)|\tilde{r}_{ui}=1} \log h'_\psi(u, i) \cdot f_\theta(u, i) - C_2 \cdot (1 - f_\theta(u, i)), \end{aligned} \quad (16)$$

where  $C_2$  is a large positive hyperparameter to replace  $-\log(h_\phi(u, i))$ .

In the training procedure of DPI and DVAE, we will expand  $E[\log P(\tilde{\mathbf{R}}|\mathbf{R})]$  as Eq.(15) and Eq.(16) iteratively to denoise both noisy positive examples and noisy negative examples. The detailed training pseudo-code of DPI and DVAE can be found in the supplement.

**Table 1.** Statistics of the datasets

Dataset	# Users	# Items	# Interactions	Sparsity
Modcloth	44783	1020	99893	0.99781
Adressa	212231	6596	419491	0.99970
Electronics	1157633	9560	1292954	0.99988

## 4 EXPERIMENTS

In this section, we instantiate the proposed DPI and DVAE with four state-of-the-art recommendation models as the target model  $f$  and conduct experiments<sup>2</sup> on three real-world datasets to verify the effectiveness of our methods. We aim to answer the following research questions:

- **RQ1:** How do DPI and DVAE perform compared to normal training and other denoising methods? Can DPI and DVAE help to downgrade the effect of noisy examples?
- **RQ2:** How does the design of DPI and DVAE affect the recommendation performance, including the iterative training and model selection?
- **RQ3:** Can DPI and DVAE generate reasonable preference distribution given the corrupted binary data observation?

### 4.1 Experimental Settings

**4.1.1 Datasets.** We conduct experiments with three public accessible datasets: Modcloth, Adressa<sup>3</sup> and Electronics<sup>4</sup>. More statistics about these three datasets are listed in Table 1. For each dataset, we construct the clean test set with only clean examples which denote the real user preference.

**Modcloth.** It is from an e-commerce website which sells women’s clothing and accessories. For evaluation, the clean test set is built on user-item pairs whose rating scores are equal to 5.

**Adressa.** This is a real-world news reading dataset from Adressavisen [11]. It contains the interaction records of anonymous users and the news. According to [20], we use interactions with dwell time longer than 10 seconds to construct the clean test set.

**Electronics.** Electronics is collected from the *Electronics* category on Amazon [27, 33]. The clean test set are built with user-item pairs with rating scores equal to 5.

Note that all the ratings and dwell time are only used to construct the clean test set. The models are trained with only the corrupted binary implicit feedback.

**4.1.2 Evaluation protocols.** We adopt cross-validation to evaluate the performance. For Adressa, we split the user-item interactions into the training set, validation set, and test set according to the ratio of 8:1:1 in chronological order due to the timeliness of news [34]. As for the other two datasets, we randomly split the historical interactions according to the ratio of 8:1:1. After that, the clean test set is constructed for

each dataset as described in section 4.1.1. The performance is measured by two widely used top- $K$  recommendation metrics [14, 40]: recall@ $K$  and ndcg@ $K$ . By default, we set  $K = 5, 20$  for Modcloth and Adressa, and  $K = 10, 50$  for Electronics since the number of items in Electronics is larger. All experiments are run 3 times and the average is reported.

**4.1.3 Baselines.** We select four state-of-the-art recommendation models as the target model  $f$  of DPI and DVAE:

- **GMF [14]:** This is a generalized version of MF by changing the inner product to the element-wise product and a dense layer.
- **NeuMF [14]:** The method is a state-of-the-art neural CF model which combines GMF with a Multi-Layer Perceptron (MLP).
- **CDAE [39]:** CDAE corrupts the observed interactions with random noises, and then employs several linear layers to reconstruct the original datasets, which will increase its anti-noise abilities.
- **LightGCN [13]:** LightGCN is a newly proposed graph-based recommendation model which learns user and item embeddings by linearly propagating them on the interaction graph.

Each model is trained with the following approaches:

- **Normal:** Train the model with the assumption shown in Figure 1(a) and simple binary-cross-entropy (BCE) loss.
- **WBPR [10]:** This is a re-sampling based denoising method, which considers the popular but uninteracted items are highly likely to be real negative.
- **T-CE [34]:** This is a re-weighting based denoising method, which uses the Truncated BCE to assign zero weights to large-loss examples with a dynamic threshold in each iteration.
- **DPI and DVAE:** Our proposed denoising methods.

Besides, [42] proposed a noisy robust learning method. We do not compare with this method because it has been shown to be only applicable to the MF model [42].

**4.1.4 Parameter settings.** We optimize all models using Adam optimizer. Batch size is set as 2048 and learning rate is set as 0.001 on all three datasets. For each training instance, we sample one interacted sample and one randomly sampled missing interaction to feed the model. We use the default network settings of all models. Besides, the embedding size of users and items in GMF and NeuMF, the hidden size of CDAE, are all set to 32. For LightGCN, the embedding size is set to 64 without dropout [13]. The  $L_2$  regularization coefficient is tuned in  $\{0.01, 0.1, 1, 10, 100, 1000\}$  divided by the number of users in each dataset. For DPI and DVAE, there are three hyper-parameters in total:  $C_1$ ,  $C_2$  and  $\alpha$ . We apply a grid search for hyperparameters:  $C_1$  and  $C_2$  are searched among  $\{1, 10, 100, 1000\}$ ,  $\alpha$  is tuned in  $\{0, 0.5, 1\}$ . Note that the hyperparameters of recommendation models keeps exactly

<sup>2</sup>The code and data are provided in [https://drive.google.com/drive/folders/1PTHYSIWb7CiE6XGednxG5vwD5XGw4\\_?usp=sharing](https://drive.google.com/drive/folders/1PTHYSIWb7CiE6XGednxG5vwD5XGw4_?usp=sharing)

<sup>3</sup><https://www.adressa.no/>

<sup>4</sup><https://www.amazon.com/>

**Table 2.** Overall performance comparison. The highest scores are in Boldface. R is short for Recall and N is short for NDCG.

Modcloth	R@5	R@20	N@5	N@20	R@5	R@20	N@5	N@20
	GMF				NeuMF			
Normal	0.063±0.006	0.225±0.008	0.043±0.005	0.088±0.005	0.082±0.003	0.242±0.004	0.055±0.002	0.101±0.002
WBPR	0.067±0.002	0.224±0.002	0.046±0.001	0.090±0.001	0.092±0.001	0.247±0.020	0.064±0.001	0.108±0.006
T-CE	0.067±0.004	0.235±0.002	0.045±0.003	0.093±0.001	0.065±0.010	0.228±0.008	0.044±0.010	0.091±0.008
DPI	0.072±0.001	0.245±0.001	0.050±0.001	0.099±0.001	<b>0.099±0.005</b>	<b>0.268±0.006</b>	<b>0.065±0.001</b>	<b>0.113±0.001</b>
DVAE	<b>0.074±0.001</b>	<b>0.247±0.001</b>	<b>0.052±0.001</b>	<b>0.100±0.000</b>	0.087±0.005	0.265±0.006	0.059±0.004	0.110±0.004
	CDAE				LightGCN			
Normal	0.082±0.004	0.242±0.003	0.052±0.002	0.098±0.001	0.065±0.001	0.220±0.002	0.043±0.001	0.087±0.002
WBPR	0.079±0.000	0.238±0.004	0.050±0.000	0.095±0.001	0.072±0.001	0.222±0.002	0.046±0.001	0.088±0.001
T-CE	0.075±0.003	0.243±0.008	0.048±0.002	0.096±0.002	0.071±0.000	0.231±0.001	0.049±0.000	0.093±0.000
DPI	0.086±0.004	0.250±0.003	0.056±0.001	0.102±0.000	0.064±0.001	0.221±0.002	0.041±0.000	0.085±0.000
DVAE	<b>0.089±0.004</b>	<b>0.251±0.005</b>	<b>0.057±0.003</b>	<b>0.103±0.003</b>	<b>0.073±0.001</b>	<b>0.235±0.001</b>	<b>0.051±0.001</b>	<b>0.096±0.000</b>
Adressa	R@5	R@20	N@5	N@20	R@5	R@20	N@5	N@20
	GMF				NeuMF			
Normal	0.116±0.003	0.209±0.005	0.080±0.002	0.112±0.001	0.169±0.004	0.312±0.004	0.131±0.002	0.180±0.003
WBPR	0.115±0.007	0.210±0.007	0.084±0.003	0.116±0.003	0.172±0.002	0.311±0.003	0.132±0.001	0.181±0.001
T-CE	0.109±0.000	0.209±0.001	0.070±0.000	0.104±0.000	0.172±0.003	0.312±0.003	0.134±0.001	<b>0.183±0.002</b>
DPI	0.119±0.002	0.218±0.001	0.090±0.001	0.125±0.001	0.170±0.006	<b>0.318±0.002</b>	0.130±0.001	0.181±0.000
DVAE	<b>0.123±0.005</b>	<b>0.220±0.001</b>	<b>0.093±0.004</b>	<b>0.127±0.003</b>	<b>0.183±0.009</b>	0.316±0.004	<b>0.137±0.002</b>	0.181±0.005
	CDAE				LightGCN			
Normal	0.162±0.000	0.317±0.001	<b>0.123±0.000</b>	0.178±0.000	0.085±0.004	0.215±0.005	0.064±0.003	0.107±0.003
WBPR	0.161±0.001	0.315±0.005	0.121±0.002	0.173±0.004	0.118±0.003	0.211±0.006	0.089±0.002	0.119±0.004
T-CE	0.161±0.001	0.317±0.003	0.122±0.002	0.176±0.004	0.119±0.001	0.206±0.003	<b>0.091±0.001</b>	0.121±0.001
DPI	0.162±0.000	0.319±0.000	0.123±0.000	0.178±0.000	0.112±0.001	0.221±0.001	0.077±0.005	0.116±0.005
DVAE	<b>0.163±0.000</b>	<b>0.320±0.002</b>	0.123±0.000	<b>0.178±0.001</b>	<b>0.121±0.001</b>	<b>0.222±0.001</b>	0.089±0.001	<b>0.125±0.000</b>
Electronics	R@10	R@50	N@10	N@50	R@10	R@50	N@10	N@50
	GMF				NeuMF			
Normal	0.023±0.000	0.063±0.001	0.013±0.000	0.021±0.000	0.075±0.000	0.191±0.002	0.048±0.000	0.072±0.001
WBPR	0.026±0.001	0.072±0.001	0.014±0.000	0.024±0.000	<b>0.077±0.000</b>	<b>0.201±0.001</b>	<b>0.048±0.000</b>	<b>0.074±0.000</b>
T-CE	0.024±0.000	0.063±0.001	0.013±0.000	0.022±0.000	0.071±0.004	0.189±0.008	0.045±0.002	0.071±0.003
DPI	<b>0.045±0.001</b>	0.104±0.000	0.023±0.000	0.037±0.000	0.071±0.001	0.191±0.001	0.044±0.002	0.069±0.001
DVAE	0.042±0.001	<b>0.110±0.000</b>	<b>0.024±0.000</b>	<b>0.038±0.000</b>	0.074±0.002	0.200±0.001	0.047±0.000	0.074±0.000
	CDAE				LightGCN			
Normal	0.074±0.001	0.197±0.001	0.047±0.000	0.073±0.000	0.024±0.000	0.081±0.001	0.016±0.000	0.030±0.000
WBPR	0.077±0.000	0.190±0.000	0.048±0.000	0.072±0.000	0.022±0.000	0.076±0.001	0.015±0.000	0.028±0.000
T-CE	0.067±0.002	0.147±0.010	0.044±0.001	0.061±0.003	0.024±0.001	0.086±0.001	0.017±0.000	0.031±0.000
DPI	<b>0.077±0.000</b>	0.201±0.001	0.048±0.000	0.075±0.000	0.022±0.000	0.097±0.001	0.015±0.000	0.033±0.000
DVAE	0.077±0.000	<b>0.202±0.001</b>	<b>0.048±0.000</b>	<b>0.075±0.000</b>	<b>0.026±0.001</b>	<b>0.104±0.001</b>	<b>0.019±0.000</b>	<b>0.037±0.000</b>

the same across all training approaches for a fair comparison. We use MF as  $h$  and  $h'$  in Eq.(2) without special mention.

#### 4.2 Performance Comparison (RQ1)

Table 2 shows the performance comparison on three datasets Modcloth, Adressa and Electronics. From the table, we can have following observations:

- The proposed DPI and DVAE can effectively improve the recommendation performance of all the four recommenders over all three datasets. Either DPI or DVAE achieves the best performance compared with normal training and other denoising methods, except for few cases and the

NeuMF model on Electronics, in which WBPR achieves the best performance.

- DPI and DVAE achieve relatively small improvements when using CDAE as the target recommendation model. The reason is that CDAE itself is based on the denoising auto-encoder which is more robust to corrupted data. However, there still exist improvements when training with our proposed methods.
- The performance of LightGCN is not so good on the three datasets. This could be attributed to the bias of datasets. We can see from Table 1 that users in the three datasets would only be connected to a small number of items while

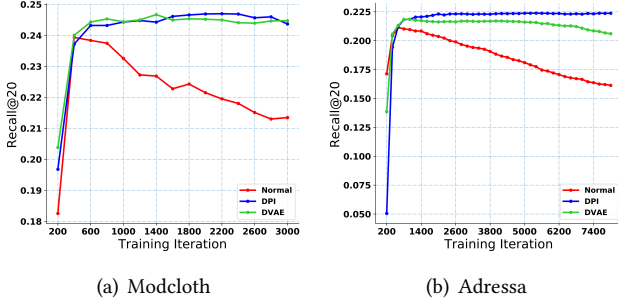


Figure 3. Recall along the training process

items are connected to a large amount of users. The imbalance of interaction graphs could affect the performance of LightGCN.

To conclude, the proposed DPI and DVAE achieve consistent and significant improvements compared with the normal training over all recommendation models. This demonstrates the effectiveness and the generalization ability of our methods.

Besides, we also analyse how DPI and DVAE affect the memorization of noisy samples. Figure 3 shows the learning curve of normal training and the proposed DPI and DVAE on Modcloth and Adressa when using GMF as the target recommender. Results on Electronics are provided in the supplement. We can see that in normal training, performance on the clean test set decreases in the late training stage. The reason is as the training goes on, the model tends to memorize all samples in the dataset, both noisy ones and clean ones. However, we can see that both DPI and DVAE remain more stable and better performance along the whole training stage. The results demonstrate that the proposed DPI and DVAE successfully prevent the model from being affected by noisy samples.

### 4.3 Model Investigation (RQ2)

**4.3.1 Ablation Study.** DPI and DVAE utilize an iterative train routine which contains two sub-tasks DP and DN. In this part, we discuss how these two sub-tasks contribute to the whole framework and how they perform separately. The results on Modcloth dataset are shown in Table 3. We can have following observations:

- In most cases, DPI and DVAE are better than only considering one sub-task of denoising. Some abnormal cases could be attributed to the instability of DN. During each training epoch, the interacted samples are fixed while the sampled negative instances could change frequently. Since DN aims to denoise noisy negative examples from the sampled missing interactions, the performance of DN could be unstable.
- DP is almost always better than DN. This observation in some extent indicates that finding noisy examples from interacted samples is much easier than finding potential

positive preference from the massive uninteracted missing samples.

**4.3.2 Hyperparameter Study.** In this part, we conduct experiments to show the effect of  $C_1$  and  $C_2$ , which are two hyper-parameters used in the iterative training routine. More specifically, a larger  $C_1$  means we are more confident that the negative samples are truly negative. A larger  $C_2$  denotes that an interacted sample is more likely to be real positive. Figure 4 shows the results on Adressa when using GMF as the target recommendation model. Results on the other datasets are provided in the supplement. From figure 4, we can find that in most cases, best performance lies in the setting  $C_1 = 1000$  and  $C_2 = 10$ . This observation indicates that the probability that a missing interaction is real negative is larger than the probability that an interacted sample is real positive.

**4.3.3 Effect of Model Selection.** We use MF as  $h$  and  $h'$  to model the probability  $P(\tilde{\mathbf{R}}|\mathbf{R})$  as our default settings. Since the model capability of MF might be limited, in this part we conduct experiments to see how the performance would be if we use more complicated models for  $h$  and  $h'$ . Table 4 shows the result on Modcloth. Results on other datasets are provided in the supplement. The target recommendation model is GMF. We can see that replacing MF with more complicated models will not boost the performance significantly. The reason might be that modelling the probability  $P(\tilde{\mathbf{R}}|\mathbf{R})$  is not a very complex task. Accomplishing this task with MF already works well. Besides, as we can see that no matter what model we use, the performance of proposed DPI and DVAE are significantly better than normal training.

### 4.4 Method Interpretation (RQ3)

In this part, we conduct experiments to see whether DPI and DVAE generate the reasonable user preference distribution given the corrupted data, which can be used to show the interpretability of our methods. For DPI, we have the following equation:

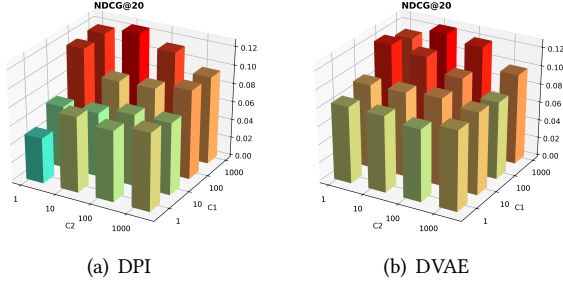
$$\begin{aligned} P(r_{ui} = 1 | \tilde{r}_{ui} = 1) &= \frac{P(\tilde{r}_{ui} = 1 | r_{ui} = 1)P(r_{ui} = 1)}{P(\tilde{r}_{ui} = 1)} \\ &= \frac{h'_{\psi}(u, i)f_{\theta}(u, i)}{h'_{\psi}(u, i)f_{\theta}(u, i) + h_{\phi}(u, i)(1 - f_{\theta}(u, i))} \end{aligned}$$

For DVAE,  $P(r_{ui} = 1 | \tilde{r}_{ui} = 1)$  can be directly computed as  $P(r_{ui} = 1 | \tilde{r}_{ui} = 1) = f_{\theta}(u, i)$  with condition  $\tilde{r}_{ui} = 1$ .  $P(r_{ui} = 1 | \tilde{r}_{ui} = 1)$  describes the probability of an interacted sample to be real positive. Figure 5 shows the relationship between ratings and mean real positive probability (i.e.,  $P(r_{ui} = 1 | \tilde{r}_{ui} = 1)$ ) on Modcloth dataset. Results on Electronics are shown in the supplement. We can see that the probability gets larger as the ratings go higher, which is consistent with the impression that examples with higher ratings should be more likely to be real positive. Besides, we can see that the probability trend is consistent with different  $h$



**Table 3.** Performance comparison when considering one sub-task. DPI-DP and DPI-DN denote training DPI with only either DP or DN. DVAE-DP and DVAE-DN denote training DVAE with only either DP or DN.

	GMF				NeuMF				CDAE				LightGCN			
	R@5	R@20	N@5	N@20	R@5	R@20	N@5	N@20	R@5	R@20	N@5	N@20	R@5	R@20	N@5	N@20
DPI-DP	0.072	0.245	0.050	0.098	0.089	0.256	0.061	0.109	0.077	0.236	0.050	0.095	0.066	0.223	0.042	0.086
DPI-DN	0.051	0.187	0.032	0.071	0.045	0.198	0.027	0.070	0.066	0.236	0.044	0.093	<b>0.068</b>	<b>0.240</b>	<b>0.047</b>	<b>0.096</b>
DPI	<b>0.072</b>	<b>0.245</b>	<b>0.050</b>	<b>0.099</b>	<b>0.099</b>	<b>0.268</b>	<b>0.065</b>	<b>0.113</b>	<b>0.086</b>	<b>0.250</b>	<b>0.056</b>	<b>0.102</b>	0.064	0.221	0.041	0.085
DVAE-DP	<b>0.075</b>	0.243	0.052	0.099	<b>0.094</b>	<b>0.268</b>	<b>0.064</b>	<b>0.113</b>	<b>0.091</b>	0.245	<b>0.059</b>	0.102	0.065	0.220	0.042	0.086
DVAE-DN	0.060	0.221	0.039	0.084	0.092	0.255	0.062	0.108	0.073	0.238	0.050	0.097	0.072	<b>0.240</b>	0.049	0.096
DVAE	0.074	<b>0.247</b>	<b>0.052</b>	<b>0.100</b>	0.087	0.265	0.059	0.110	0.089	<b>0.251</b>	0.057	<b>0.103</b>	<b>0.073</b>	0.235	<b>0.051</b>	<b>0.096</b>

**Figure 4.** Hyperparameter study on Adressa.**Table 4.** Effect of model selection on Modcloth.

Method	$h$ and $h'$	R@5	R@20	N@5	N@20
Normal		0.0629	0.2246	0.0430	0.0884
DPI	MF	0.0717	0.2452	0.0500	0.0985
	GMF	0.0740	0.2453	0.0513	0.0989
	NeuMF	0.0747	0.2448	0.0519	0.0991
DVAE	MF	0.0743	0.2465	0.0515	0.0996
	GMF	0.0740	0.2464	0.0508	0.0989
	NeuMF	0.0751	0.2464	0.0514	0.0992

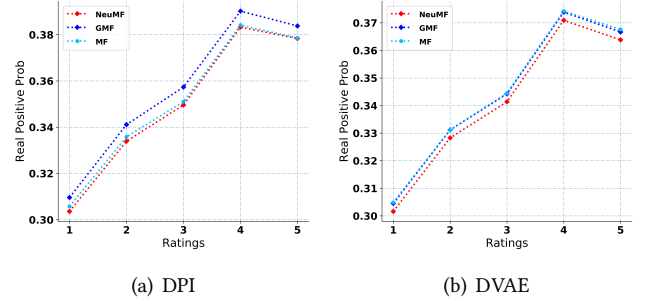
and  $h'$  models, which further demonstrate the generalization ability of our methods.

## 5 Related Work

In this section, we provide a literature review about implicit feedback recommendation and existing denoising methods.

### 5.1 Implicit Feedback Recommendation

Modern recommender systems are usually trained using implicit feedback data. The training of implicit recommenders usually needs to sample negative examples from missing interactions and then feed the interacted items and sampled negative instances for pair-wise ranking [28] or BCE loss function. Besides, there are also attempts to investigate non-sampling approaches [1, 15, 44] for implicit feedback. Regarding the recommendation models, MF [21] is one of the most notable and effective models, which projects users and items to embedding vectors and then calculate the inner product between them as the prediction score. Recently, plenty of work has proposed deep learning-based recommendation models, such as GMF, NeuMF[14], CDAE[39]

**Figure 5.** Mean real positive probability of different ratings on Modcloth. Model names in the legend denote different  $h$  and  $h'$ .

and Wide&Deep [3]. The key idea is to use deep learning to increase model expressiveness to capture more complex signals. Besides, graph neural networks also demonstrated their capability in recommendation. Plenty of models have emerged, such as HOP-Rec [40], KGAT [35], NGCF [36] and LightGCN [13]. This work aims at developing denoising learning methods which can be used to train various kinds of models, other than a specific recommendation model.

### 5.2 Denoising in Recommendation

In recently years, there has been some research [18, 24] pointing out that the observed implicit feedback could be easily corrupted by different factors, such as popularity bias, conformity bias, exposure bias and position bias[2]. Training recommenders with corrupted implicit data would lead to misunderstanding of the real user preference and sub-optimal recommendation performance [34, 45]. As a result, there have been some efforts aiming to address the noisy problem, which can be categorized into re-sampling methods [5–7, 9, 42], re-weighting methods [26, 30, 34] and methods utilizing additional knowledge input [20, 25, 45]. Re-sampling methods aim to design more effective samplers for implicit feedback. For example, [9] proposed to sample popular but not interacted items as negative examples while [5] proposed that the viewed but not purchased items are highly likely to be real negative. [6, 37] proposed to use reinforcement learning for negative sampling. The performance of re-sampling depends heavily on the sampling strategy [44], which is usually developed heuristically [42]. Re-weighting methods

usually identify the noisy examples as samples with high loss values and then assign lower weights to them. But the denoising signal contained in loss values could encounter difficulties to distinguish noisy samples and hard clean samples [31]. Besides, additional knowledge such as dwell time [20], gaze pattern [45] and auxiliary item features [25] can also be used to denoise implicit feedback, which, however, is usually expensive to collect.

## 6 Conclusion

In this work, we propose probabilistic and variational recommendation denoising for implicit feedback. We find that different models or one model trained with different random seeds tend to make more consistent predictions for clean examples compared with the noisy ones. To this end, we propose two denoising learning frameworks DPI and DVAE, which utilize predictions from different models or one model with different random seeds as the denoising signal. We employ DPI and DVAE on four state-of-the-art recommendation models and conduct extensive experiments on three real-world datasets. The results demonstrate the effectiveness of our methods. To the best of our knowledge, this is the first paper to consider the variance between different models as the denoising signal, and it's also the first work to denoise both noisy positive examples and noisy negative examples. Future work includes using DPI and DVAE for other domain applications, such as image classification on corrupted labels. Besides, we are also interested in generalizing DPI and DVAE for multi-class denoising scenario.

## References

- [1] Chong Chen, Min Zhang, Chenyang Wang, Weizhi Ma, Minming Li, Yiqun Liu, and Shaoping Ma. 2019. An efficient adaptive transfer neural network for social-aware recommendation. In *SIGIR*. 225–234.
- [2] Jiawei Chen, Hande Dong, Xiang Wang, Fuli Feng, Meng Wang, and Xiangnan He. 2020. Bias and Debias in Recommender System: A Survey and Future Directions. *arXiv preprint arXiv:2010.03240* (2020).
- [3] Heng-Tze Cheng, Levent Koc, Jeremiah Harmsen, Tal Shaked, Tushar Chandra, Hrishi Aradhye, Glen Anderson, Greg Corrado, Wei Chai, Mustafa Ispir, et al. 2016. Wide & deep learning for recommender systems. In *Proceedings of the 1st workshop on deep learning for recommender systems*. 7–10.
- [4] James Davidson, Benjamin Liebald, Junning Liu, Palash Nandy, Taylor Van Fleet, Ullas Gargi, Sujoy Gupta, Yu He, Mike Lambert, Blake Livingston, et al. 2010. The YouTube video recommendation system. In *Proceedings of the fourth ACM conference on Recommender systems*. 293–296.
- [5] Jingtao Ding, Fuli Feng, Xiangnan He, Guanghui Yu, Yong Li, and Depeng Jin. 2018. An improved sampler for bayesian personalized ranking by leveraging view data. In *Companion Proceedings of the The Web Conference 2018*. 13–14.
- [6] Jingtao Ding, Yuhuan Quan, Xiangnan He, Yong Li, and Depeng Jin. 2019. Reinforced Negative Sampling for Recommendation with Exposure Data.. In *IJCAI*. 2230–2236.
- [7] Jingtao Ding, Guanghui Yu, Xiangnan He, Fuli Feng, Yong Li, and Depeng Jin. 2019. Sampler design for bayesian personalized ranking by leveraging view data. *IEEE Transactions on Knowledge and Data Engineering* (2019).
- [8] Carl Doersch. 2016. Tutorial on variational autoencoders. *arXiv preprint arXiv:1606.05908* (2016).
- [9] Zeno Gantner, Lucas Drumond, Christoph Freudenthaler, and Lars Schmidt-Thieme. 2012. Personalized ranking for non-uniformly sampled items. In *Proceedings of KDD Cup 2011*. PMLR, 231–247.
- [10] Zeno Gantner, Lucas Drumond, Christoph Freudenthaler, and Lars Schmidt-Thieme. 2012. Personalized ranking for non-uniformly sampled items. In *Proceedings of KDD Cup 2011*. PMLR, 231–247.
- [11] Jon Atle Gulla, Lemei Zhang, Peng Liu, Özlem Özgöbek, and Xiaomeng Su. 2017. The Adressa dataset for news recommendation. In *Proceedings of the international conference on web intelligence*. 1042–1048.
- [12] Bo Han, Quanming Yao, Xingrui Yu, Gang Niu, Miao Xu, Weihua Hu, Ivor Tsang, and Masashi Sugiyama. 2018. Co-teaching: Robust training of deep neural networks with extremely noisy labels. In *Proceedings of the 32nd Conference on Neural Information Processing Systems*.
- [13] Xiangnan He, Kuan Deng, Xiang Wang, Yan Li, Yongdong Zhang, and Meng Wang. 2020. Lightgcn: Simplifying and powering graph convolution network for recommendation. In *Proceedings of the 43rd International ACM SIGIR Conference on Research and Development in Information Retrieval*. 639–648.
- [14] Xiangnan He, Lizi Liao, Hanwang Zhang, Liqiang Nie, Xia Hu, and Tat-Seng Chua. 2017. Neural collaborative filtering. In *Proceedings of the 26th international conference on world wide web*. 173–182.
- [15] Xiangnan He, Hanwang Zhang, Min-Yen Kan, and Tat-Seng Chua. 2016. Fast matrix factorization for online recommendation with implicit feedback. In *Proceedings of the 39th International ACM SIGIR conference on Research and Development in Information Retrieval*. 549–558.
- [16] Matthew D Hoffman, David M Blei, Chong Wang, and John Paisley. 2013. Stochastic variational inference. *Journal of Machine Learning Research* 14, 5 (2013).
- [17] Yifan Hu, Yehuda Koren, and Chris Volinsky. 2008. Collaborative filtering for implicit feedback datasets. In *2008 Eighth IEEE International Conference on Data Mining*. Ieee, 263–272.
- [18] Rolf Jagerman, Harrie Oosterhuis, and Maarten de Rijke. 2019. To model or to intervene: A comparison of counterfactual and online learning to rank from user interactions. In *Proceedings of the 42nd International ACM SIGIR Conference on Research and Development in Information Retrieval*. 15–24.
- [19] Lu Jiang, Zhengyuan Zhou, Thomas Leung, Li-Jia Li, and Li Fei-Fei. 2018. Mentornet: Learning data-driven curriculum for very deep neural networks on corrupted labels. In *International Conference on Machine Learning*. PMLR, 2304–2313.
- [20] Youngho Kim, Ahmed Hassan, Ryan W White, and Imed Zitouni. 2014. Modeling dwell time to predict click-level satisfaction. In *Proceedings of the 7th ACM international conference on Web search and data mining*. 193–202.
- [21] Yehuda Koren, Robert Bell, and Chris Volinsky. 2009. Matrix factorization techniques for recommender systems. *Computer* 42, 8 (2009), 30–37.
- [22] Tzu-Heng Lin, Chen Gao, and Yong Li. 2019. Cross: Cross-platform recommendation for social e-commerce. In *Proceedings of the 42nd International ACM SIGIR Conference on Research and Development in Information Retrieval*. 515–524.
- [23] Chao Liu, Ryan W White, and Susan Dumais. 2010. Understanding web browsing behaviors through Weibull analysis of dwell time. In *Proceedings of the 33rd international ACM SIGIR conference on Research and development in information retrieval*. 379–386.
- [24] Hongyu Lu, Min Zhang, and Shaoping Ma. 2018. Between clicks and satisfaction: Study on multi-phase user preferences and satisfaction for online news reading. In *The 41st International ACM SIGIR Conference on Research & Development in Information Retrieval*. 435–444.
- [25] Hongyu Lu, Min Zhang, Weizhi Ma, Ce Wang, Feng xia, Yiqun Liu, Leyu Lin, and Shaoping Ma. 2019. Effects of User Negative Experience in Mobile News Streaming. In *Proceedings of the 42nd International*

- ACM SIGIR Conference on Research and Development in Information Retrieval. 705–714.
- [26] Duc Tam Nguyen, Chaithanya Kumar Mummadi, Thi Phuong Nhung Ngo, Thi Hoai Phuong Nguyen, Laura Beggel, and Thomas Brox. 2019. Self: Learning to filter noisy labels with self-ensembling. *arXiv preprint arXiv:1910.01842* (2019).
  - [27] Jianmo Ni, Jiacheng Li, and Julian McAuley. 2019. Justifying recommendations using distantly-labeled reviews and fine-grained aspects. In *Proceedings of the 2019 Conference on Empirical Methods in Natural Language Processing and the 9th International Joint Conference on Natural Language Processing (EMNLP-IJCNLP)*. 188–197.
  - [28] Steffen Rendle, Christoph Freudenthaler, Zeno Gantner, and Lars BPR Schmidt-Thieme. 2014. Bayesian personalized ranking from implicit feedback. In *Proc. of Uncertainty in Artificial Intelligence*. 452–461.
  - [29] Steffen Rendle, Walid Krichene, Li Zhang, and John Anderson. 2020. Neural collaborative filtering vs. matrix factorization revisited. In *Recsys*. 240–248.
  - [30] Yanyao Shen and Sujay Sanghavi. 2019. Learning with bad training data via iterative trimmed loss minimization. In *International Conference on Machine Learning*. PMLR, 5739–5748.
  - [31] Jun Shu, Qi Xie, Lixuan Yi, Qian Zhao, Sanping Zhou, Zongben Xu, and Deyu Meng. 2019. Meta-weight-net: Learning an explicit mapping for sample weighting. In *Proceedings of 33rd Conference on Neural Information Processing Systems*.
  - [32] Aäron Van Den Oord, Sander Dieleman, and Benjamin Schrauwen. 2013. Deep content-based music recommendation. In *Neural Information Processing Systems Conference (NIPS 2013)*, Vol. 26. Neural Information Processing Systems Foundation (NIPS).
  - [33] Mengting Wan, Jianmo Ni, Rishabh Misra, and Julian McAuley. 2020. Addressing Marketing Bias in Product Recommendations. In *Proceedings of the 13th International Conference on Web Search and Data Mining*. 618–626.
  - [34] Wenjie Wang, Fuli Feng, Xiangnan He, Liqiang Nie, and Tat-Seng Chua. 2020. Denoising Implicit Feedback for Recommendation. In *Proceedings of the 14th ACM International Conference on Web Search and Data Mining*.
  - [35] Xiang Wang, Xiangnan He, Yixin Cao, Meng Liu, and Tat-Seng Chua. 2019. Kgat: Knowledge graph attention network for recommendation. In *Proceedings of the 25th ACM SIGKDD International Conference on Knowledge Discovery & Data Mining*. 950–958.
  - [36] Xiang Wang, Xiangnan He, Meng Wang, Fuli Feng, and Tat-Seng Chua. 2019. Neural graph collaborative filtering. In *Proceedings of the 42nd international ACM SIGIR conference on Research and development in Information Retrieval*. 165–174.
  - [37] Xiang Wang, Yaokun Xu, Xiangnan He, Yixin Cao, Meng Wang, and Tat-Seng Chua. 2020. Reinforced negative sampling over knowledge graph for recommendation. In *Proceedings of The Web Conference 2020*. 99–109.
  - [38] Hongyi Wen, Longqi Yang, and Deborah Estrin. 2019. Leveraging post-click feedback for content recommendations. In *Recsys*. 278–286.
  - [39] Yao Wu, Christopher DuBois, Alice X Zheng, and Martin Ester. 2016. Collaborative denoising auto-encoders for top-n recommender systems. In *Proceedings of the Ninth ACM International Conference on Web Search and Data Mining*. 153–162.
  - [40] Jheng-Hong Yang, Chih-Ming Chen, Chuan-Ju Wang, and Ming-Feng Tsai. 2018. HOP-rec: high-order proximity for implicit recommendation. In *Recsys*. 140–144.
  - [41] Xing Yi, Liangjie Hong, Erheng Zhong, Nanthan Nan Liu, and Suju Rajan. 2014. Beyond clicks: dwell time for personalization. In *Proceedings of the 8th ACM Conference on Recommender systems*. 113–120.
  - [42] Wenhui Yu and Zheng Qin. 2020. Sampler Design for Implicit Feedback Data by Noisy-label Robust Learning. In *Proceedings of the 43rd International ACM SIGIR Conference on Research and Development in Information Retrieval*. 861–870.
  - [43] Fajie Yuan, Guibing Guo, Joemon M Jose, Long Chen, Haitao Yu, and Weinan Zhang. 2016. Lambdafm: learning optimal ranking with factorization machines using lambda surrogates. In *Proceedings of the 25th ACM International on Conference on Information and Knowledge Management*. 227–236.
  - [44] Fajie Yuan, Xin Xin, Xiangnan He, Guibing Guo, Weinan Zhang, Chua Tat-Seng, and Joemon M Jose. 2018. fbgd: Learning embeddings from positive unlabeled data with bgd. In *UAI*.
  - [45] Qian Zhao, Shuo Chang, F Maxwell Harper, and Joseph A Konstan. 2016. Gaze prediction for recommender systems. In *Recsys*. 131–138.

## A Supplement

### A.1 Pseudo-code for DPI and DVAE

---

**Algorithm 1:** Learning algorithm for DPI
 

---

**Input:** Corrupted data  $\tilde{\mathbf{R}}$ , learning rate  $\beta$ , epochs  $T$ , hyper-parameter  $\alpha, C_1, C_2$ , regularization weight  $\lambda$ , target recommender  $f$ , auxiliary model  $g, h, h'$

**Output:** Parameters  $\theta, \mu, \phi, \psi$  for  $f, g, h, h'$ , correspondingly

```

1 Initialize all parameters;
2  $count \leftarrow 0$ ;
3 while Not early stop and epoch  $< T$  do
4   Draw a minibatch of  $(u, i_+)$  from  $\{(u, i) | \tilde{r}_{ui} = 1\}$ ;
5   Draw  $(u, i_-)$  from  $\{(u, i) | \tilde{r}_{ui} = 0\}$  for each  $(u, i_+)$ ;
6   if  $count \% 2 == 0$  then
7     Compute  $\mathcal{L}_{DPI}$  according to Eq.(9) and Eq.(15);
8   else
9     Compute  $\mathcal{L}_{DPI}$  according to Eq.(9) and Eq.(16);
10    Add regularization term:  $\mathcal{L}_{DPI} \leftarrow \mathcal{L}_{DPI} + \lambda ||\theta||^2$ ;
11    for each parameter  $\Theta$  in  $\{\theta, \mu, \phi, \psi\}$  do
12      Compute  $\partial \mathcal{L}_{DPI} / \partial \Theta$  by back-propagation;
13       $\Theta \leftarrow \Theta - \beta \partial \mathcal{L}_{DPI} / \partial \Theta$ 
14    end
15     $count \leftarrow count + 1$ ;
16 end
```

---

**Algorithm 2:** Learning algorithm for DVAE
 

---

**Input:** Corrupted data  $\tilde{\mathbf{R}}$ , learning rate  $\beta$ , epochs  $T$ , hyper-parameter  $\alpha, C_1, C_2$ , regularization weight  $\lambda$ , target recommender  $f$ , auxiliary model  $h, h'$

**Output:** Parameters  $\theta, \phi, \psi$  for  $f, h, h'$ , correspondingly

```

1 Set random seed to  $s_1$ , initialize another copy of  $\theta$  as  $\theta'$ ;
2 while Not early stop and epoch  $< T$  do
3   Draw a minibatch of  $(u, i_+)$  from  $\{(u, i) | \tilde{r}_{ui} = 1\}$ ;
4   Draw  $(u, i_-)$  from  $\{(u, i) | \tilde{r}_{ui} = 0\}$  for each  $(u, i_+)$ ;
5   Compute binary cross-entropy  $\mathcal{L}_{BCE}$  on  $(u, i_+)$  and  $(u, i_-)$  with  $f_{\theta'}$ ;
6   Add regularization:  $\mathcal{L}_{BCE} \leftarrow \mathcal{L}_{BCE} + \lambda ||\theta'||^2$ ;
7   Compute  $\partial \mathcal{L}_{BCE} / \partial \theta'$  by back-propagation;
8    $\theta' \leftarrow \theta' - \beta \partial \mathcal{L}_{BCE} / \partial \theta'$ ;
9 end
10 Freeze  $\theta'$ , set random seed to  $s_2$  and initialize  $\theta, \phi, \psi$ ;
11  $count \leftarrow 0$ ;
12 while Not early stop and epoch  $< T$  do
13   Draw  $(u, i_+)$  and  $(u, i_-)$  similarly with line3-4;
14   if  $count \% 2 == 0$  then
15     Compute  $\mathcal{L}_{DVAE}$  according to Eq.(14) and Eq.(15);
16   else
17     Compute  $\mathcal{L}_{DVAE}$  according to Eq.(14) and Eq.(16);
18     Add regularization term:  $\mathcal{L}_{DVAE} \leftarrow \mathcal{L}_{DVAE} + \lambda ||\theta||^2$ ;
19     for each parameter  $\Theta$  in  $\{\theta, \phi, \psi\}$  do
20       Compute  $\partial \mathcal{L}_{DVAE} / \partial \Theta$  by back-propagation;
21        $\Theta \leftarrow \Theta - \beta \partial \mathcal{L}_{DVAE} / \partial \Theta$ ;
22     end
23      $count \leftarrow count + 1$ ;
24 end
```

---

### A.2 Supplementary Results

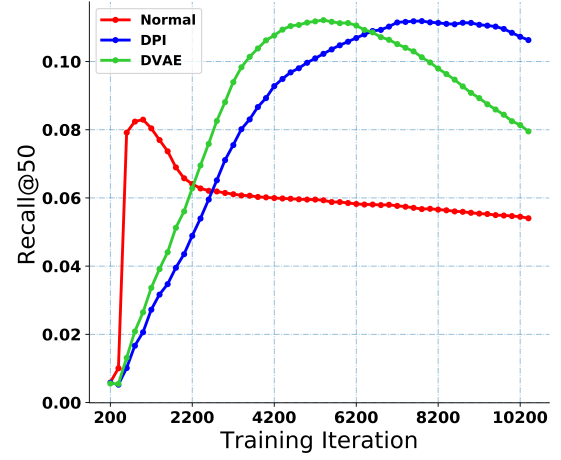


Figure 6. Recall along the training process on Electronics.

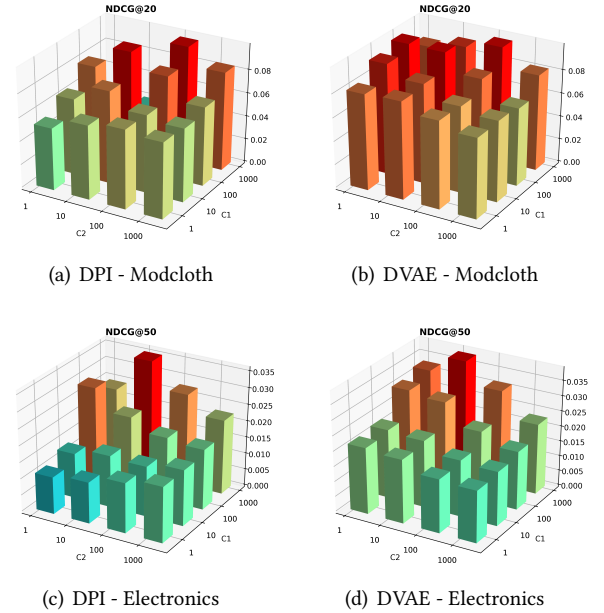


Figure 7. Hyperparameter study on Modcloth and Electronics.

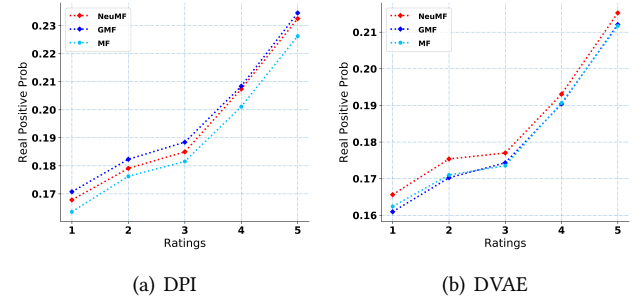


**Table 5.** Effect of model selection on Adressa.

Method	$h$ and $h'$	R@5	R@20	N@5	N@20
Normal		0.1163	0.2089	0.0801	0.1125
DPI	MF	0.1190	0.2182	0.0904	0.1250
	GMF	0.1179	0.2188	0.0906	0.1255
	NeuMF	0.1208	0.2197	0.0913	0.1255
DVAE	MF	0.1233	0.2203	0.0932	0.1270
	GMF	0.1221	0.2182	0.0912	0.1245
	NeuMF	0.1216	0.2178	0.0906	0.1240

**Table 6.** Effect of model selection on Electronics.

Method	$h$ and $h'$	R@10	R@50	N@10	N@50
Normal		0.0227	0.0633	0.0128	0.0214
DPI	MF	0.0451	0.1040	0.0234	0.0365
	GMF	0.0447	0.1047	0.0235	0.0368
	NeuMF	0.0447	0.1042	0.0233	0.0365
DVAE	MF	0.0411	0.1102	0.0222	0.0372
	GMF	0.0428	0.1125	0.0235	0.0386
	NeuMF	0.0429	0.1115	0.0237	0.0386

**Figure 8.** Mean real positive probability of different ratings on Electronics. Model names in the legend denote different  $h$  and  $h'$ .